HIF2α inhibition promotes p53 pathway activity, tumor cell death, and radiation responses

Jessica A. Bertout[a,b,c], Amar J. Majmundar[a,b,d], John D. Gordan[a,b,d], Jennifer C. Lam[a,b,e], Dara Ditsworth[a,b,d], Brian Keith[a,b,d], Eric J. Brown[a,b,d], Katherine L. Nathanson[b,d,f], and M. Celeste Simon[a,b,d,e,1]

[a]Abramson Family Cancer Research Institute, [b]Abramson Cancer Center, [c]School of Veterinary Medicine, [d]School of Medicine, [f]Department of Medicine, and [e]Howard Hughes Medical Institute, University of Pennsylvania, Philadelphia, PA 19104.

Communicated by Craig B. Thompson, University of Pennsylvania, Philadelphia, PA, July 9, 2009 (received for review November 21, 2008)

Approximately 50% of cancer patients receive radiation treatment, either alone or in combination with other therapies. Tumor hypoxia has long been associated with resistance to radiation therapy. Moreover, the expression of hypoxia inducible factors HIF1α and/or HIF2α correlates with poor prognosis in many tumors. Recent evidence indicates that HIF1α expression can enhance radiation-induced apoptosis in cancer cells. We demonstrate here that HIF2α inhibition promotes tumor cell death and, in contrast to HIF1α, enhances the response to radiation treatment. Specifically, inhibiting HIF2α expression augments p53 activity, increases apoptosis, and reduces clonogenic survival of irradiated and non-irradiated cells. Moreover, HIF2α inhibition promotes p53-mediated responses by disrupting cellular redox homeostasis, thereby permitting reactive oxygen species (ROS) accumulation and DNA damage. These results correlate with altered p53 phosphorylation and target gene expression in untreated human tumor samples and show that HIF2α likely contributes to tumor cell survival including during radiation therapy.

cancer | ROS | IR | Hypoxia | DNA Damage

Many cellular responses to hypoxia are mediated by the hypoxia inducible factors (HIFs). These transcription factors promote the expression of over 200 genes (1) and are heterodimers consisting of either HIF1α or HIF2α bound to the HIFβ/ARNT subunit. While ARNT is constitutively expressed, both HIFα subunits are regulated by O_2 availability. Under normoxia, the von Hippel–Lindau (VHL) E3 ligase complex targets HIFα subunits for proteasomal degradation (2). When O_2 levels decline, the HIFα subunits are stabilized, bind ARNT, and activate the expression of target genes providing hypoxic adaptations.

Solid tumors are characterized by oncogenic signaling and hypoxic microenvironments that promote HIFα accumulation (3). Moreover, HIF1α and/or HIF2α expression has been associated with increased tumor vascularization and poor prognosis of numerous cancers such as breast, ovarian, and non-small cell lung cancer (2, 4). Of note, in mouse xenograft models, HIF2α (and not HIF1α) expression is crucial for growth of clear cell renal cell carcinoma (ccRCC) (5, 6) and neuroblastoma (7) tumors.

TP53 is a tumor suppressor that is mutated or silenced in a majority of human cancers (8). It coordinates many cellular stress responses by regulating genes involved in DNA repair, cell cycle arrest, and apoptosis. Following stress stimuli, p53 is activated through a variety of post-translational modifications, including phosphorylation on serine 15 (9). For example, the ataxia telangiectasia mutated (ATM) and checkpoint kinase 2 (Chk2) kinases directly phosphorylate p53 in response to DNA damage, resulting in its activation (9). Although many tumors select for *TP53* mutations, p53 pathway inhibition can also contribute to tumor progression (10).

With the emergence of HIF inhibitors (11, 12) and their potential use in cancer therapy, it is important to accurately predict the response of HIFα-expressing tumor cells to treatment. HIF1α appears to enhance p53 activation by γ-radiation (IR), resulting in increased p53 phosphorylation and p53-induced apoptosis (13). Furthermore, HIF1α has been shown to complex with p53 and promote its stability (14, 15). In contrast, a role for HIF2α in p53 pathway regulation and cellular responses to IR has not been reported. It is becoming increasingly clear that HIF1α and HIF2α can have distinct effects in tumor cells (6, 16). As HIF2α inhibits reactive oxygen species (ROS) accumulation in other contexts (17), we hypothesized that HIF2α suppresses p53 activation by reducing ROS levels generated from normal metabolic processes as well as IR treatment, promoting tumor cell survival.

We report here that HIF2α deficiency promotes p53 phosphorylation in ccRCC and lung carcinoma cells in culture. Importantly, HIF2α expression correlates with decreased p53 phosphorylation and target gene expression in human ccRCC tumor samples. HIF2α knockdown results in increased p53 transcriptional activity and cell death before and after IR in ccRCC cells. HIF2α-deficient cells exhibit increased ATM activity and DNA double strand break formation, as well as elevated ROS levels after IR. Treatment with an ATM inhibitor or the antioxidant butyl-hydroxyanisole (BHA) largely rescues the p53 phenotype, supporting our model that HIF2α regulates p53 responses by controlling ROS accumulation. Finally, microarray analysis identified a number of HIF2α target genes with antioxidant function. In summary, HIF2α inhibition enhances ccRCC cell death by disrupting cellular redox balance, thereby promoting DNA damage.

Results

HIF2α Deficiency Promotes p53 Activation. To assess the effect of HIF2α on the p53 pathway, we selected two *VHL*-deficient human ccRCC cell lines that express HIF2α (A498 and 786-O) under normoxic conditions (18). These cell lines do not produce HIF1α and harbor a wild-type *TP53* allele (NCI-60 cell line database, 19). We also chose these lines to avoid the confounding factors of HIF1α and pVHL expression, described to promote p53 stabilization and activity (20). Using siRNA, we achieved 80–90% HIF2α knockdown in A498 cells (Fig. 1*A* and Fig. 2*A* inset). We probed immunoblots for either total p53 or p53 phosphorylated at serine 15 (pS15-p53), an IR-induced modification associated with increased p53 activity. Compared to controls, HIF2α knockdown led to elevated baseline pS15-p53, which was increased upon exposure to 2 and 10 Gray (Gy) IR (Fig. 1*A*). Concomitantly, we observed increases in baseline p53 protein levels, which were augmented by IR. These results suggested that HIF2α expression correlates with decreased pS15-p53 and total p53 protein levels in both untreated and IR-treated A498 cells. Of note, the effects were observed with two independent siRNAs (Fig. S1*A*), which were then used in combination for subsequent experiments. Similar results were

Author contributions: J.A.B., J.D.G., E.J.B., K.L.N., and M.C.S. designed research; J.A.B., A.J.M., J.D.G., and J.C.L. performed research; D.D., E.J.B., K.L.N., and M.C.S. contributed new reagents/analytic tools; J.A.B., A.J.M., J.D.G., J.C.L., D.D., B.K., E.J.B., K.L.N., and M.C.S. analyzed data; and J.A.B., A.J.M., B.K., and M.C.S. wrote the paper.

The authors declare no conflict of interest.

Freely available online through the PNAS open access option.

[1]To whom correspondence should be addressed. E-mail: celeste2@mail.med.upenn.edu.

This article contains supporting information online at www.pnas.org/cgi/content/full/0907357106/DCSupplemental.

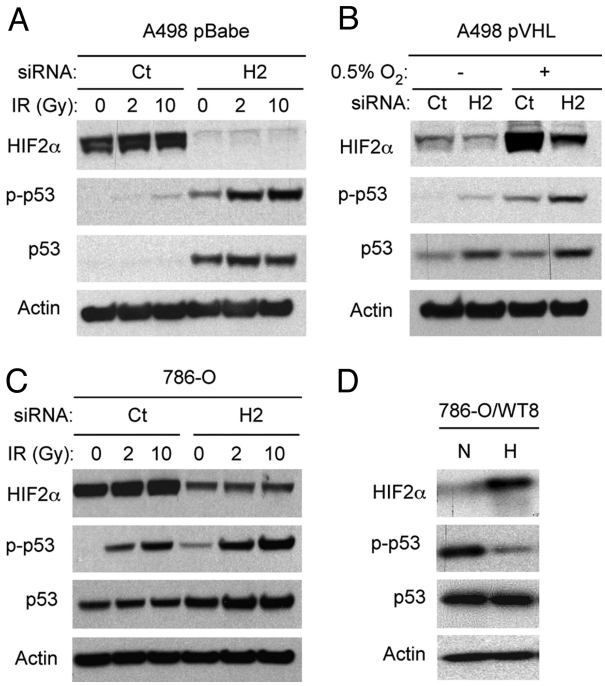

Fig. 1. HIF2α deficiency promotes p53 phosphorylation. Representative western blots of HIF2α, pS15-p53, p53, and actin protein in: (*A*) A498 cells stably transduced with empty vector pBabe and treated with control (Ct) or HIF2α (H2) siRNA for 48 h before indicated doses of IR and harvest 1 h after IR, (*B*) A498 cells transduced with wild-type pVHL and treated with siRNA for 24 h before being exposed to 21% or 0.5% O_2 for 48 h, (*C*) 786-O cells harboring empty vector pRc/CMV2 treated with siRNA for 48 h before indicated doses of IR and harvest 1 h after IR, and (*D*) 786-O cells transduced with wild-type pVHL (786-O/WT8) and exposed to 21% or 0.5% O_2 for 24 h.

obtained using 786-O cells (Fig. 1*C*). Moreover, we observed that HIF2α loss promoted p53 pathway activation in the presence of the pan caspase inhibitor Q-VD-OPh (Fig. S1*B*), indicating that p53 activation was not secondary to cell death.

To determine if HIF2α's effects occur in a *VHL* wild-type background, we used A498 cells in which human *VHL* cDNA has been stably reintroduced ("A498 pVHL"). HIF2α knockdown promoted p53 phosphorylation and increased p53 protein levels in A498 pVHL cells under both normoxic (21%) and hypoxic conditions (0.5% O_2) (Fig. 1*B*), suggesting that low levels of HIF2α are sufficient to mediate these effects. Interestingly, 786-O cells that stably express human *VHL* ("786-O/WT8 cells") cultured at 0.5% O_2 for 24 h exhibited HIF2α stabilization and a concomitant reduction of pS15-p53 (Fig. 1*D*). This finding was further confirmed with wild-type HIF2α overexpression in normoxic 786-O and 786-O/WT8 cells (Fig. S1 *C* and *D*).

Finally, to extend our studies to non-renal cells, we used A549 cells, a wild-type *TP53* human lung adenocarcinoma cell line (NCI-60 database) that expresses wild-type pVHL, HIF1α, and HIF2α (21). In these cells, HIF2α knockdown resulted in significant increases in p53 protein levels and pS15-p53 (Fig. S1*E*). We concluded that HIF2α's effects on p53 are not limited to ccRCC or cancer cells exclusively expressing HIF2α.

HIF2α Inhibition Promotes p53 Target Expression, Cell Death, and Cell Cycle Arrest. We next investigated the cellular outcome of HIF2α-mediated p53 inhibition. Transcript levels for several p53 targets were measured in irradiated and non-irradiated A498 cells treated with HIF2α siRNA. IR-treated control cells showed only minor increases in Bax, Noxa, and 14–3-3σ mRNAs, and modest but reproducible increases in Puma and MDM2 expression (Fig. 2*A*). Compared to control cells, however, HIF2α knockdown cells showed a marked increase in 14–3-3σ (5-fold), Puma (3-fold), and MDM2 (2-fold) mRNAs and a subtle increase in Bax transcripts, while the expression of Noxa (Fig. 2*A*) and a number of other known p53 targets (Fig. S2*A*) did not change significantly. Microarray analysis (see below) revealed increased expression of additional p53 targets (22), including *XPC* (q = 3.77), p53 apoptosis effector related to PMP-22 (q = 6.27), *TP53IP* (q = 2.28), *TRIAP1* (q = 6.27), and cell death-inducing protein (q = 5.03).

Consistent with the QRT-PCR data, HIF2α knockdown led to a 4-fold increase in 14–3-3σ and a 2.5-fold increase in Puma protein levels by immunoblot (Fig. 2*B* and Fig. S2*B*). In addition, changes in Puma expression correlated with a 5-fold increase in caspase 3 cleavage in response to 10 Gy IR (Fig. 2*B*). Elevated cleaved caspase 3 levels were also observed in non-irradiated HIF2α deficient cells relative to controls (Fig. S2*B*). These data suggest that HIF2α inhibits the expression of a subset of p53 target genes involved in apoptosis and cell cycle arrest. Moreover, HIF2α's effects on 14–3-3σ, Puma, and caspase 3 cleavage were abrogated by p53 knockdown and are thus p53-dependent (Fig. 2*B*).

We next investigated whether HIF2α inhibition promotes cell death. HIF2α knockdown led to a 3-fold increase in baseline subG1 DNA content (5.3% in control cells versus 17.9% in H2 knockdown cells), consistent with decreased viability (Fig. 2*C*). Twenty-four hours after 2 Gy IR exposure, 4.6-fold more HIF2α depleted cells were detected in subG1 relative to controls (29.9% vs. 6.4% subG1) (Fig. 2*C*). While additional increases in the percent of HIF2α-deficient cells in subG1 were not observed after 10 Gy IR, significantly more HIF2α knockdown cells were in subG1 than controls (23.7% vs. 7.7% subG1) (Fig. 2*C*). Similar increases in cell death were detected using two independent siRNAs (Fig. S3*A*). Moreover, A498 pVHL cells treated with HIF2α siRNA exhibited a statistically significant decrease in viability after 10 Gy IR under hypoxic conditions, indicating the effect of HIF2α does not require a *VHL*-deficient background (Fig. S3*B*).

Interestingly, HIF2α loss also promoted accumulation of cells in G2/M after IR. Using BrdU incorporation, the number of HIF2α-deficient cells in the G2/M phase of the cell cycle was significantly increased 24 h after 2 and 10 Gy of IR (Fig. 2*D* and Fig. S3*C* box).

To assess the effects of HIF2α loss on tumor cell cycle progression and cell death beyond 24 h, we performed a clonogenic survival assay. After 11 days in culture, HIF2α deficiency led to a 4.9-fold decrease in mean survival fraction (SF)—an established measure of colony formation. HIF2α depletion also enhanced radiation treatment as evidenced by 6.1- and 8.6-fold lower survival fractions at 2 and 10 Gy IR, respectively (Fig. 2 *E* and *F* and Fig. S3*D*). The effect of HIF2α loss on SF was statistically significant by two-way ANOVA ($P < 0.0001$). To adjust for the effects of HIF2α deficiency without IR, mean SFs of HIF2α siRNA groups were normalized to the HIF2α siRNA/0 Gy IR SF. The resulting "H2 siRNA Normalized" curve slopes lower than the control curve (Fig. 2*F*), indicating a trend toward synergy between HIF2α inhibition and radiation therapy.

HIF2α Deficiency Promotes DNA Damage Accumulation. HIF2α inhibition promotes p53 pathway activity; we therefore sought to delineate mechanisms underlying these effects. As HIF2α is a transcription factor, we measured p53 mRNA levels in A498 cells treated with control or HIF2α siRNA for 48 h (Fig. S4). HIF2α depletion resulted in a subtle increase in p53 mRNA levels, but this change was not statistically significant.

As ATM is the kinase that primarily mediates immediate IR-induced pS15-p53, we assessed its contribution to the p53 phenotype observed in HIF2α deficient cells. An ATP-competitive inhibitor of ATM abolished IR-induced pS15-p53 (Fig. 3*A*) as well as Chk2 phosphorylation (Fig. S5*A*), impairing ATM activity. Of note, this inhibitor also largely eliminated the effect of HIF2α knockdown on total p53 protein levels in both A498 (Fig. 3*A*) and 786-O

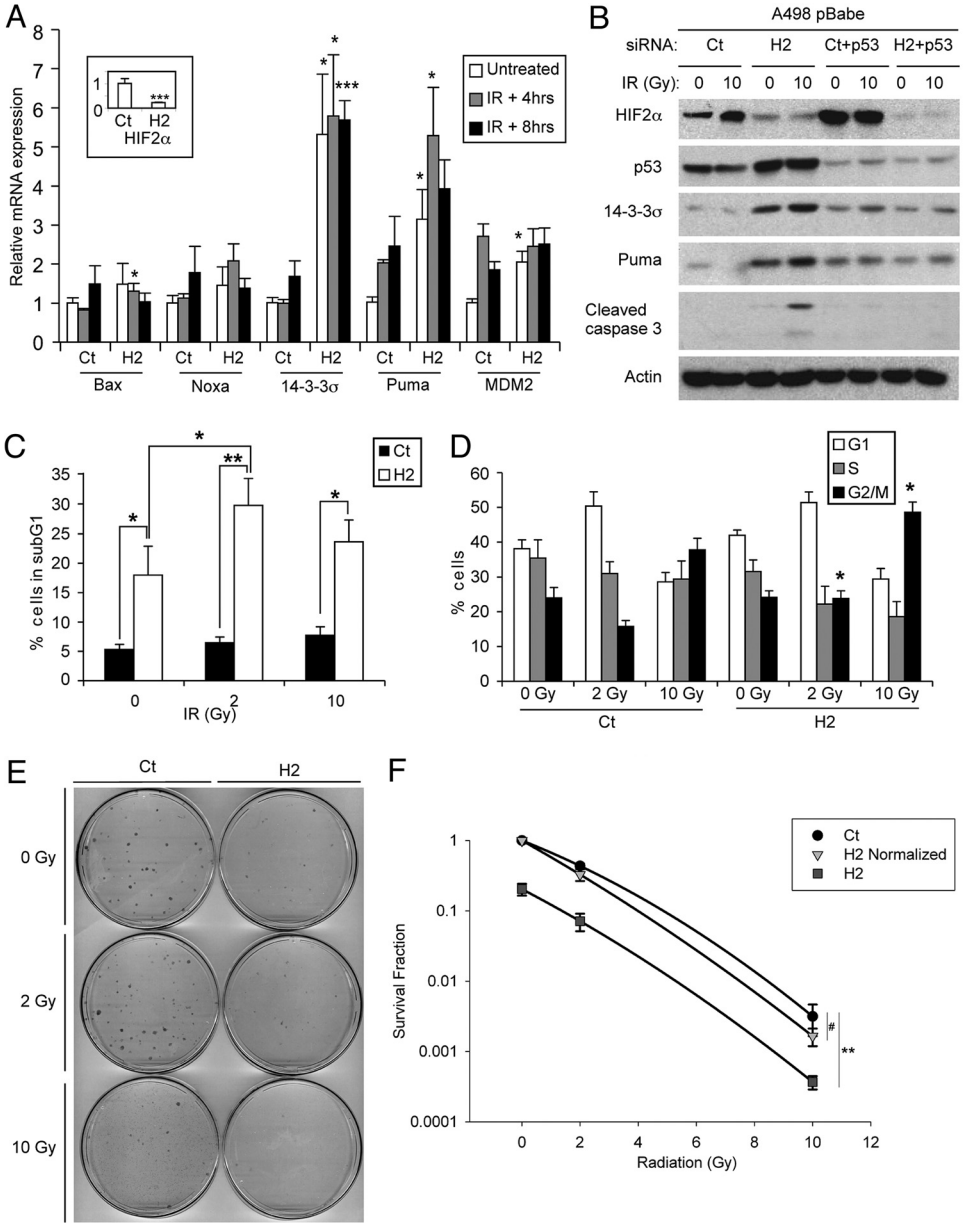

Fig. 2. HIF2α deficiency promotes p53 target gene expression, cell death, cell cycle arrest, and clonogenicity. (*A*) mRNA expression of HIF2α and p53 targets in A498 cells after 48 h treatment with Ct or HIF2α siRNA followed by 10 Gy IR. RNA was harvested 4–8 h after IR. mRNA expression was measured by QRT-PCR and averaged from four experiments; error bars, ± 1 SEM. *, $P < 0.05$, ***, $P < 0.001$. (*B*) Representative western blot of p53 target expression in A498 cells with p53 knockdown. Cells were treated with the indicated siRNA for 48 h, irradiated, and harvested 24 h after IR. (*C*) Summary of changes in subG1 populations in siRNA-treated A498 cells 24 h after IR. Results averaged from three to five experiments; error bars, ± 1 SEM. *, $P < 0.05$, **, $P < 0.0005$. (*D*) Average BrdU cell cycle analysis of siRNA-treated A498 cells 24 h after IR; error bars, ± 1 SEM. *, $P < 0.05$ (comparing H2 to Ct cells). (*E*) Representative examples of clonogenic assays stained with Wright-Giemsa. (*F*) Graph of mean survival fraction (SF) as a function of radiation for control (CT) or HIF2α (H2) siRNA-treated A498 cells. Included also is H2 normalized data. Data points averaged from three to five experiments; error bars, ± 1 SEM. #, $P = 0.1035$, **, $P < 0.0001$

cells (Fig. S5*B*). Using the ATM/ATR inhibitor CGK733, we then assessed the contribution of ataxia telangiectasia and Rad3-related (ATR) kinase, which also regulates p53-mediated DNA damage responses. CGK733 reduced IR-induced pS15-p53 and Chk2 phosphorylation (Fig. S5 *A* and *C*) and suppressed the effect of HIF2α knockdown on pS15-p53 and total p53 in both A498 and 786-O cell lines (Fig. S5 *C* and *D*). However, effects on p53 with the ATM-specific inhibitor and the ATM/ATR inhibitor were quantitatively similar. This suggested that while ATR may play a minor role in p53 protein level changes, ATM is responsible for the majority of the phenotype. Consistent with this mechanism, Chk2 phosphorylation was increased in HIF2α knockdown A498 cells (Fig. 3*B*), while HIF2α overexpression in 786-O cells (Fig. 3*C*) reduced Chk2 phosphorylation. We concluded that HIF2α knockdown cells may have elevated levels of DNA damage resulting in increased ATM pathway activity.

DNA double strand breaks (DSBs) stimulate the formation of nuclear foci containing the phosphorylated histone variant H2AX (γH2AX), a direct target of ATM. The number of γH2AX foci was increased by HIF2α depletion in A498 and 786-O cells, consistent with increased DSBs before and after IR (Fig. 3 *D–F*). We directly tested this possibility using pulsed-field gel electrophoresis (PFGE), which separates large DNA fragments from chromosomal DNA to allow visualization of DSBs. In HIF2α depleted A498 cells, PFGE revealed an 2.7-fold increase in basal levels of DSBs as well as a 3-fold increase in DSBs immediately after irradiation (Fig. 3*G*). These DSBs were largely repaired after 2 h recovery. We concluded that HIF2α inhibits DNA damage accumulation, which may explain the commonly observed radioresistance of human ccRCCs.

HIF2α Deficiency Activates p53 by Enhancing ROS Accumulation. Previous studies suggested that HIF2α regulates the expression of specific antioxidant genes (17). Given that IR damages cells by promoting ROS accumulation, we compared ROS levels in control and HIF2α knockdown A498 cells using dichlorofluorescein diacetate (DCFDA), a cell permeable dye that fluoresces in response to increased cellular oxidation (Fig. 4 *A* and *B*). Significantly more

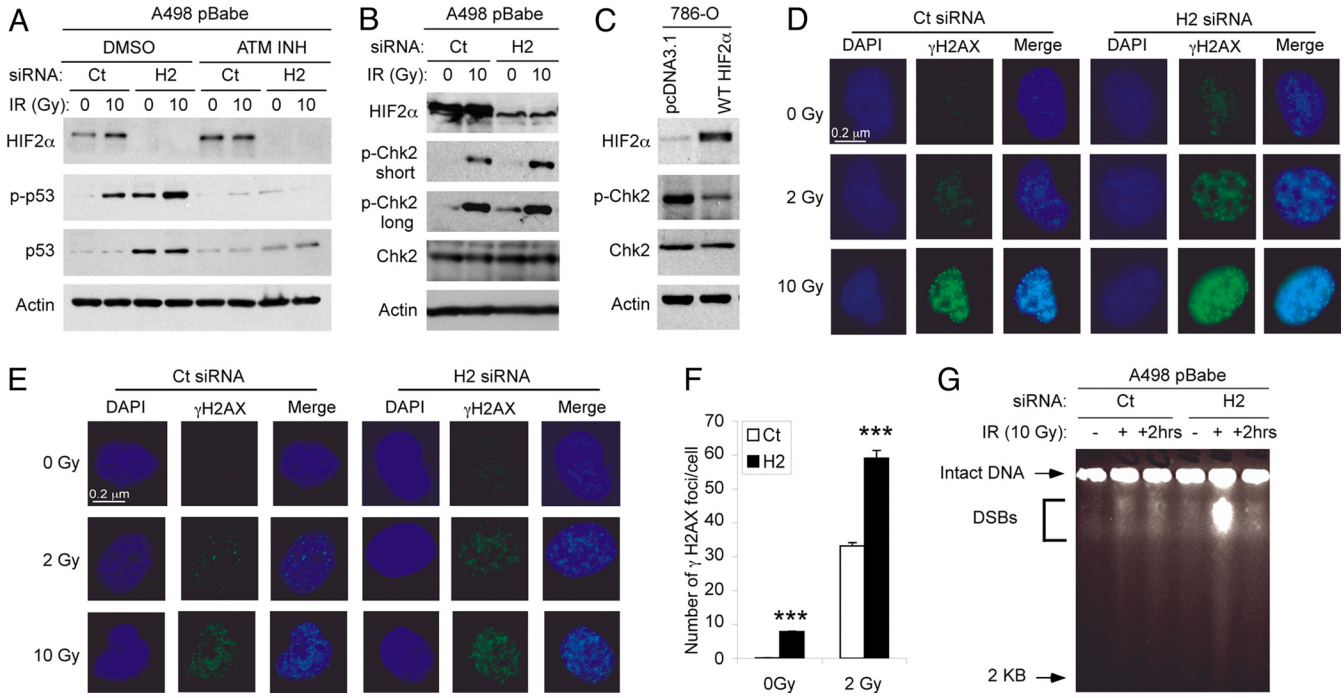

Fig. 3. HIF2α deficiency promotes DNA damage accumulation. (*A*) Western blot of p53 phosphorylation and protein levels in A498 cells after ATM inhibition. Cells were transfected with HIF2α or Ct siRNA 16 h before treatment with 10 μM ATM inhibitor for 24 h and IR. Cells were harvested 60 min after IR. (*B*) Western blot of HIF2α, phospho-Chk2 and total Chk2 in A498 cells. Cells were treated with HIF2α or Ct siRNA for 48 h before 10 Gy IR, and harvested approximately 45 min after IR. Long and short exposures of blots are shown. (*C*) Western blot of HIF2α, phospho-Chk2 and total Chk2 in 786-O cells transfected with pcDNA3.1 or wild-type HIF2α and harvested 48 h later. (*D*) Representative immunofluorescence for γH2AX in A498 cells. Cells were treated with HIF2α or Ct siRNA for 48 h before 2 Gy IR, and then fixed and stained 15 min after IR. Quantification was not possible in A498 cells due to large numbers of merging or overlapping foci. (*E*) 786-O cells were treated as described for A498 cells in (*D*). (*F*) Quantification of γH2AX foci in Ct ($n = 54$) and HIF2α ($n = 63$) knockdown 786-O cells after 0 and 2 Gy of IR from 3 independent experiments. ***, $P < 0.0005$. Quantification was not possible after 10 Gy IR due to overlapping foci. (*G*) Representative PFGE gel showing DSBs in A498 cells. Cells were treated with HIF2α or Ct siRNA for 48 h before IR and harvest. Cells were left untreated, treated with 10 Gy IR and placed immediately on ice, or treated with 10 Gy IR and given 2 h to repair before harvest.

HIF2α deficient cells were DCFDA-positive following IR treatment than control cells, suggesting that HIF2α deficiency enhanced IR-induced ROS levels (Figs. 4 *A* and *B*). Consistent with this interpretation, treatment of A498 cells with the antioxidant BHA abrogated HIF2α effects on ROS levels (Fig. S6*A*) and reduced pS15-p53 before and after 2 Gy IR (Fig. 4*C*). Moreover, BHA also decreased total p53 protein levels in HIF2α deficient cells (Fig. 4*C*). Importantly, BHA had no reproducible effect on pS15-p53 or total p53 levels in control cells. We concluded that HIF2α inhibits p53 pathway activation by limiting ROS accumulation, thereby reducing the number of IR-induced DSBs, p53 pathway activation, and cell death.

Although HIF2α has been reported to regulate *SOD1*, *SOD2*, *Gpx1*, and *Catalase* expression (17), HIF2α inhibition did not reduce the expression of these genes in A498 cells by QRT-PCR (Fig. S6*B*). We therefore conducted microarray analysis of control and HIF2α knockdown A498 mRNA to identify HIF2α-regulated antioxidant genes. Based on microarray and QRT-PCR assays, several genes associated with antioxidant activity were expressed at lower levels in HIF2α knockdown cells (Fig. 4*D* and Fig. S6*C*): *HMOX1*, *XIAP*, *PRDX3*, *CP*, *Crystallin*, and a putative member of the glutathione peroxidase family (*GPX8*) (23–28).

Human ccRCC Samples Exclusively Expressing HIF2α Exhibit Decreased p53 Pathway Activity. Our in vitro models identified an important HIF2α inhibitory effect on p53 activity. To confirm the relevance of this finding in vivo, we assessed p53 phosphorylation and target gene expression in human ccRCC samples of similar histological grade and clinical stage, which had not received cytotoxic therapy. We observed three categories of HIFα expression in these tumors (29): *VHL* wild type with no HIFα expression ("*VHL* WT"), *VHL*-deficient tumors expressing HIF1α and HIF2α ("H1H2"), and *VHL*-deficient tumors expressing only HIF2α ("H2"). To evaluate the relationship between HIF2α and p53 phosphorylation in human renal tumors, we performed co-immunofluorescence staining on sections from 25 specimens (four *VHL* WT, 11 H1H2, and 10 H2). Representative images are shown in Fig. 5*A*. Of note, we did not detect pS15-p53 in nuclei that were γH2AX negative. Consistent with results obtained using cell lines, we observed a significant decrease in pS15-p53 and γH2AX positive nuclei in H2 tumors as compared to the other tumor subgroups (Fig. 5*B*). Furthermore, immunoblot analysis revealed decreased H2AX phosphorylation in H2 tumors relative to H1H2 samples (Fig. 5*C*). H2 tumors also exhibited increased Ki67$^+$ cells (29), indicating that reduced γH2AX staining could not be attributed to decreased proliferation.

The decreased p53 phosphorylation correlated with reduced transcriptional activity, as H2 tumors expressed lower levels of Puma mRNA than *VHL* WT and H1H2 tumors and reduced levels of 14–3-3σ mRNA compared to *VHL* WT tumors (Fig. 5*D*). Moreover, expression profiling identified *MDM2* and *TP53AP1* as additional p53 targets whose expression was decreased in H2 tumors. QRT-PCR analysis confirmed these findings (Fig. 5*E*). Consistent with this result, gene set enrichment analysis demonstrated reduced p53 activity in H2 tumors (FDR = 0.255 for a Broad Institute gene set card for p53 targets) with decreased expression of p53 targets including p21 and cathepsin D. These results indicate that HIF2α expression inhibits the p53 axis of DNA damage responses in vivo. Finally, H2 samples exhibited significantly increased expression of HMOX1, CP, and Crystallin in a

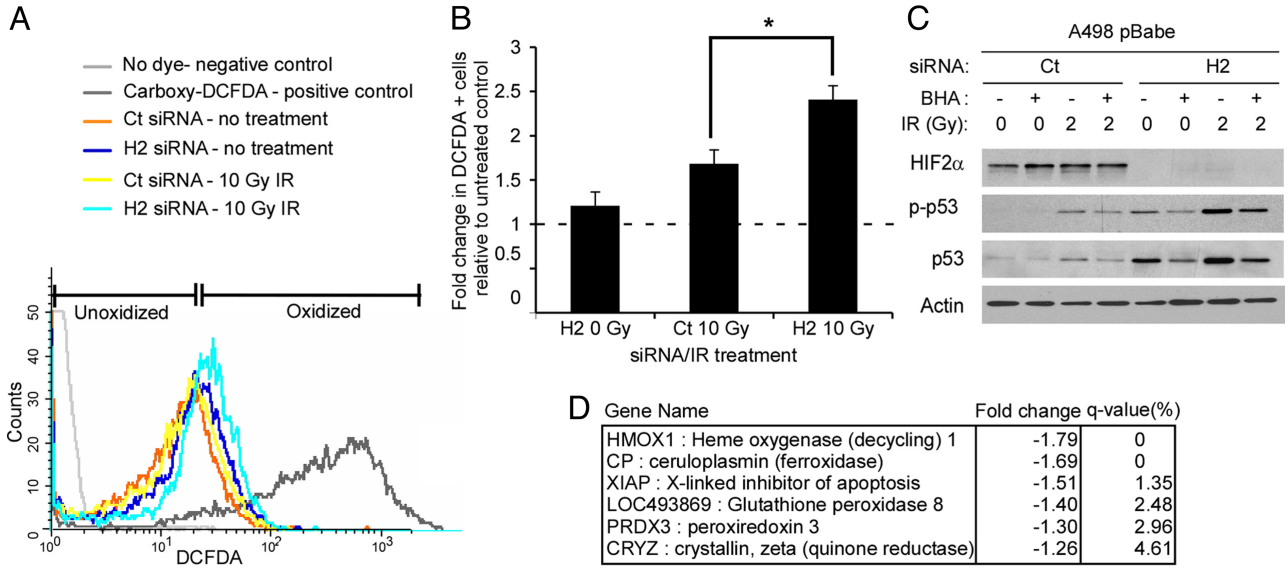

Fig. 4. HIF2α deficiency activates p53 by enhancing ROS accumulation. (*A*) Representative FACS assay showing DCFDA fluorescence in A498 cells. Cells were treated with HIF2α or Ct siRNA for 48 h before loading with DCFDA dye, IR and harvest for flow cytometry. Additional controls include cells not exposed to DCFDA dye to assess background fluorescence and cells exposed to preoxidized dye (carboxy-DCFDA) as a positive control. (*B*) Summary of three independent DCFDA staining experiments. *, $P < 0.05$ (*C*) Representative western blot of A498 cell lysates showing the effect of BHA treatment on pS15-p53 and p53 protein levels. Lysates were transfected with HIF2α or Ct siRNA 16 h before treatment with 100 μM BHA for 24 h and IR. Lysates were harvested 60 min after IR. (*D*) Genes with antioxidant activity identified by microarray analysis to exhibit reduced expression in HIF2α deficient A498 cells (q-values represent false discovery rates).

comparison of all three tumor types, further suggesting a role for HIF2α in regulating redox status and suppressing cellular responses to IR in human tumors.

Discussion

It is increasingly clear that HIF1α and HIF2α have contrasting roles in tumor cell biology, as evidenced by their opposing regulation of c-Myc (16). Dewhirst and colleagues reported that HIF1α stimulates p53 phosphorylation and p53-dependent cell death in cancer cells (13). Conversely, we demonstrate here that HIF2α inhibition promotes p53 activity.

HIF2α knockdown enhances pS15-p53 and total p53 protein levels in an ATM-dependent manner and stimulates selective p53-dependent target gene expression in tumor cell lines. These effects correlate with increased G2/M arrest, elevated levels of cell death and decreased colony formation, all of which were stimulated by IR. Of note, it is typical to observe changes in some but not all p53 targets because of factors such as cellular context, posttranslational modifications, availability of specific transcriptional cofactors, and stress category and dosage (22, 30, 31).

Next, we investigated how HIF2α affects p53. HIF2α knockdown cells exhibited decreased expression of antioxidant genes and elevated levels of ROS. Moreover, HIF2α-dependent p53 phosphorylation changes were largely rescued by antioxidant treatment. Therefore, we propose that HIF2α regulates multiple antioxidant enzymes, thereby controlling intracellular ROS levels. This regulation limits DNA damage accumulation and p53 activation. These data are consistent with prior studies of *Hif2*$\alpha^{-/-}$ mice that exhibit increased ROS and reduced levels of antioxidant enzymes (17). However, we have identified a distinct set of genes involved in redox homeostasis as HIF2α targets. Furthermore, since the ATM inhibitor did not completely rescue the p53 phenotype, we cannot exclude the involvement of other HIF2α-regulated factors affecting DNA damage levels and/or ATM activity. For example, recent evidence from our lab suggests that HIF2α also promotes the expression of several DNA damage repair enzymes (29).

Given our in vitro results, we assessed p53 phosphorylation in human ccRCC samples. H2 tumors showed reductions in γH2AX and pS15-p53, when compared to tumors expressing both H1H2 as well as *VHL* WT tumors which express neither. Furthermore, H2 samples exhibited reduced expression of p53 targets while having increased levels of antioxidant gene products. Thus, we propose that HIF2α inhibits p53 activity in human ccRCCs by modulating cellular redox status (Fig. 5*F*). Interestingly, H1H2 tumors exhibited similar rates of p53 phosphorylation as *VHL* WT ccRCCs, suggesting that when both subunits are expressed, they counterbalance each other. It is unclear why *VHL* wild-type and H1H2 tumors expressed similar levels of Puma mRNA but different levels of 14–3-3σ; this might reflect effects of HIFα/VHL on other pathways regulating *14–3-3*σ. Whether the influences of one HIFα subunit predominate over the other will likely depend on factors such as tumor environment, O_2 availability, oncogenic signaling, and relative abundance of each HIFα protein.

Whereas HIF1α appears to promote IR sensitivity of cancer cells (13), our findings implicate HIF2α in tumor cell resistance to radiation therapy. HIF2α also affected p53 in the absence of IR, suggesting that HIF2α inhibition may be effective alone or in combination with therapies other than radiation. In addition, although HIF2α function can depend on tumor type (32), we observed similar effects of HIF2α on p53 in lung carcinoma and ccRCC. Further study is needed to evaluate whether our model applies to other cell types (i.e. non-epithelial cells) and other DNA damaging agents. These results strongly encourage the development of specific HIF2α inhibitors for use in tumors with an intact p53 stress response pathway (12).

Materials and Methods

Cell Culture. One hundred micromolar (BHA) (Calbiochem) and 10 μM ATM inhibitor (Calbiochem 118500) were used for 24 h before IR.

RNA Interference. siRNAs against HIF2α (Hs_EPAS1_2 and 4), p53 (Hs_TP53_9) and a control siRNA were obtained from Qiagen.

For additional protocols, see *SI Text*.

ACKNOWLEDGMENTS. We thank many Abramson Family Cancer Research Institute members including Roger Greenberg and Russell Jones for helpful sug-

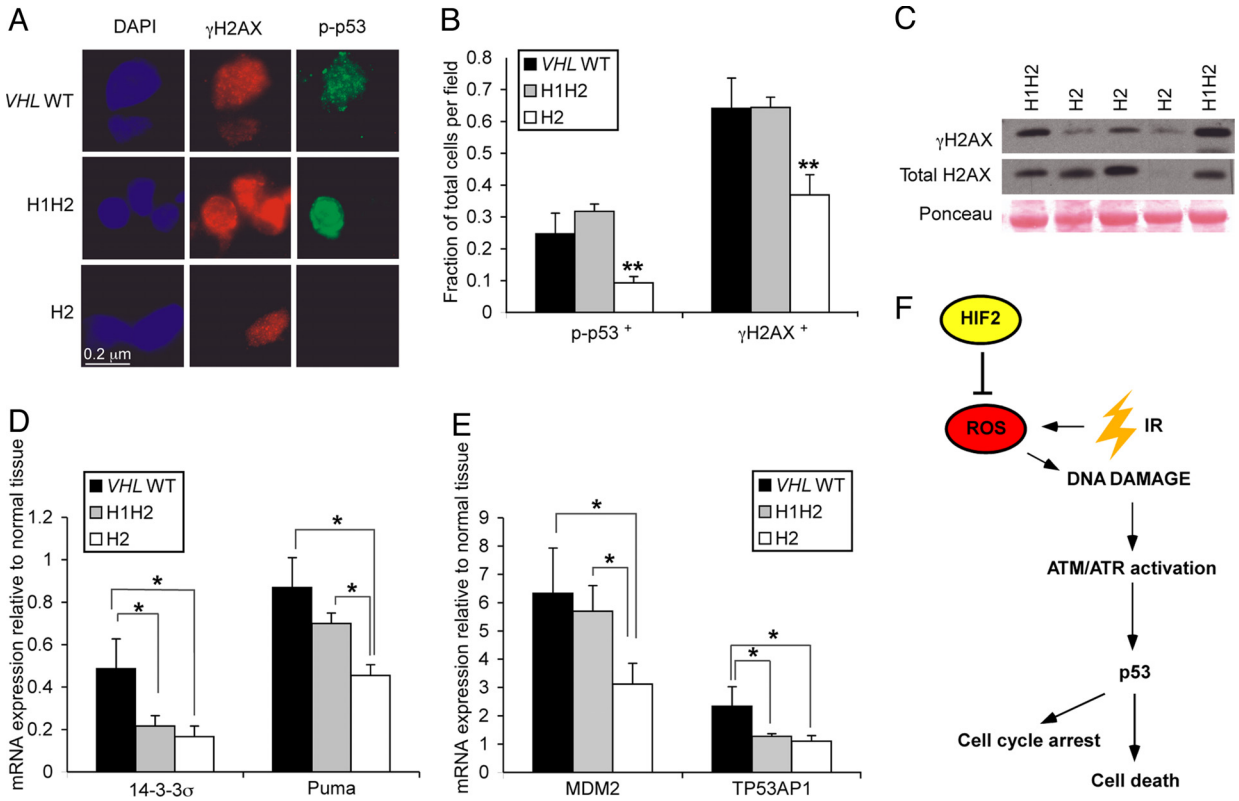

Fig. 5. Human ccRCC samples exclusively expressing HIF2α show decreased p53 activity. (*A*) Representative immunofluorescence in frozen human ccRCC samples stained with antibodies to γH2AX and pS15-p53. (*B*) Summary quantification of the percentage of cells staining positively for pS15-p53 or γH2AX in each tumor type. **, $P < 0.02$ (*C*) Western blot showing γH2AX and total H2AX in *VHL* deficient human ccRCCs. (*D*) Summary QRT-PCR data showing mRNA expression of 14–3-3σ and Puma in human ccRCCs relative to pooled normal kidney epithelial tissue. *, $P < 0.05$. (*E*) QRT-PCR data showing mRNA expression of MDM2 and TP53AP1 in human ccRCCs relative to pooled normal kidney epithelial tissue. *, $P < 0.05$. (*F*) Model for HIF2α's effects on p53 pathway activity: HIF2α inhibits the p53 pathway by modulating cellular oxidation status to limit DNA damage accumulation.

gestions; Donna George, Wafik El-Deiry, and Michael Atchison for manuscript suggestions; and Brad Johnson for use of his PFGE equipment. This work was supported by the Howard Hughes Medical Institute, National Institutes of Health Program Project Grant CA104838; ''The Training Program in Cancer Pharmacology'' from the National Cancer Institute Grant R25 CA101871; a Veterinary Scientist Training Grant and the National Cancer Institute R25 Training Grant CA101871 (to J.A.B.). M.C.S. is an Investigator of the Howard Hughes Medical Institute.

1. Gordan JD, Simon MC (2007) Hypoxia-inducible factors: Central regulators of the tumor phenotype. *Curr Opin Genet Dev* 17:71–77.
2. Bertout JA, Patel SA, Simon MC (2008) The impact of O(2) availability on human cancer. *Nat Rev Cancer* 8:967–975.
3. Pugh CW, Ratcliffe PJ (2003) Regulation of angiogenesis by hypoxia: Role of the HIF system. *Nat Med* 9:677–684.
4. Semenza GL (2003) Targeting HIF-1 for cancer therapy. *Nat Rev Cancer* 3:721–732.
5. Kondo K, Kim WY, Lechpammer M, Kaelin WG, Jr (2003) Inhibition of HIF2alpha is sufficient to suppress pVHL-defective tumor growth. *PLoS Biol* 1:E83.
6. Raval RR, et al. (2005) Contrasting properties of hypoxia-inducible factor 1 (HIF-1) and HIF-2 in von Hippel-Lindau-associated renal cell carcinoma. *Mol Cell Biol* 25:5675–5686.
7. Holmquist-Mengelbier L, et al. (2006) Recruitment of HIF-1alpha and HIF-2alpha to common target genes is differentially regulated in neuroblastoma: HIF-2alpha promotes an aggressive phenotype. *Cancer Cell* 10:413–423.
8. Hainaut P, et al. (1998) IARC Database of p53 gene mutations in human tumors and cell lines: Updated compilation, revised formats, and new visualisation tools. *Nucleic Acids Res* 26:205–213.
9. Lavin MF, Gueven N (2006) The complexity of p53 stabilization and activation. *Cell Death Differ* 13:941–950.
10. Gurova KV, Hill JE, Razorenova OV, Chumakov PM, Gudkov AV (2004) p53 pathway in renal cell carcinoma is repressed by a dominant mechanism. *Cancer Res* 64:1951–1958.
11. Melillo G (2006) Inhibiting hypoxia-inducible factor 1 for cancer therapy. *Mol Cancer Res* 4:601–605.
12. Zimmer M, et al. (2008) Small-molecule inhibitors of HIF-2a translation link its 5′UTR iron-responsive element to oxygen sensing. *Mol Cell* 32:838–848.
13. Moeller BJ, et al. (2005) Pleiotropic effects of HIF-1 blockade on tumor radiosensitivity. *Cancer Cell* 8:99–110.
14. An WG, et al. (1998) Stabilization of wild-type p53 by hypoxia-inducible factor 1alpha. *Nature* 392:405–408.
15. Sanchez-Puig N, Veprintsev DB, Fersht AR (2005) Binding of natively unfolded HIF-1alpha ODD domain to p53. *Mol Cell* 17:11–21.
16. Gordan JD, Bertout JA, Hu CJ, Diehl JA, Simon MC (2007) HIF-2alpha promotes hypoxic cell proliferation by enhancing c-myc transcriptional activity. *Cancer Cell* 11:335–347.
17. Scortegagna M, et al. (2003) Multiple organ pathology, metabolic abnormalities and impaired homeostasis of reactive oxygen species in Epas1-/- mice. *Nat Genet* 35:331–340.
18. Maxwell PH, et al. (1999) The tumour suppressor protein VHL targets hypoxia-inducible factors for oxygen-dependent proteolysis. *Nature* 399:271–275.
19. Stickle NH, et al. (2005) Expression of p53 in renal carcinoma cells is independent of pVHL. *Mutat Res* 578:23–32.
20. Roe JS, et al. (2006) p53 stabilization and transactivation by a von Hippel-Lindau protein. *Mol Cell* 22:395–405.
21. Uchida T, et al. (2004) Prolonged hypoxia differentially regulates hypoxia-inducible factor (HIF)-1alpha and HIF-2alpha expression in lung epithelial cells: Implication of natural antisense HIF-1alpha. *J Biol Chem* 279:14871–14878.
22. Vousden KH (2006) Outcomes of p53 activation–spoilt for choice. *J Cell Sci* 119:5015–5020.
23. Otterbein LE, Soares MP, Yamashita K, Bach FH (2003) Heme oxygenase-1: Unleashing the protective properties of heme. *Trends Immunol* 24:449–455.
24. Resch U, Schichl YM, Sattler S, de Martin R (2008) XIAP regulates intracellular ROS by enhancing antioxidant gene expression. *Biochem Biophys Res Commun* 375:156–161.
25. Chang TS, et al. (2004) Peroxiredoxin III, a mitochondrion-specific peroxidase, regulates apoptotic signaling by mitochondria. *J Biol Chem* 279:41975–41984.
26. Atanasiu RL, et al. (1998) Direct evidence of caeruloplasmin antioxidant properties. *Mol Cell Biochem* 189:127–135.
27. Bianco NR, Perry G, Smith MA, Templeton DJ, Montano MM (2003) Functional implications of antiestrogen induction of quinone reductase: Inhibition of estrogen-induced deoxyribonucleic acid damage. *Mol Endocrinol* 17:1344–1355.
28. Toppo S, Vanin S, Bosello V, Tosatto SC (2008) Evolutionary and structural insights into the multifaceted glutathione peroxidase (Gpx) superfamily. *Antioxid Redox Signal* 10:1501–1514.
29. Gordan JD, et al. (2008) HIF-alpha effects on c-Myc distinguish two subtypes of sporadic VHL-deficient clear cell renal carcinoma. *Cancer Cell* 14:435–446.
30. Fei P, Bernhard EJ, El-Deiry WS (2002) Tissue-specific induction of p53 targets in vivo. *Cancer Res* 62:7316–7327.
31. Hill R, Bodzak E, Blough MD, Lee PW (2008) p53 binding to the p21 promoter is dependent on the nature of DNA damage. *Cell Cycle* 7:2535–2543.
32. Acker T, et al. (2005) Genetic evidence for a tumor suppressor role of HIF-2alpha. *Cancer Cell* 8:131–141.